



Pr³⁺ doped BaO:ZnO:B₂O₃:TeO₂ glasses for laser host matrix

Rajaramakrishna RAJANAVANEETHAKRISHNA^{1,2}, Chananya WONGDEEYING^{2,3}, Patarawagee YASAKA^{2,3}, Pruittipol LIMKITJAROENORN^{2,3}, Narong SANGWARANATEE⁴, and Jakrapong KAEWKHAO^{2,3,*}

¹Department of Post Graduate & Research in Physics, The National College, Jayanagara, Bangalore 560070, India

²Centre of Excellence in Glass Technology and Materials Science, Nakhon Pathom Rajabhat University, Meuang, Nakhon Pathom, 73000, Thailand

³Physics Program, Faculty of Science and Technology, Nakhon Pathom Rajabhat University, Nakhon Pathom 73000, Thailand

⁴Applied Physics Research Group, Faculty of Science and Technology, Suan Sunandha Rajabhat University, Bangkok 10300, Thailand

*Corresponding author e-mail: jakrapong@npru.webmail.ac.th

Received date:

15 May 2018

Revised date:

7 June 2018

Accepted date:

12 October 2018

Keywords:

Glasses
FTIR studies
XRD
Optical properties
Luminescence properties

Abstract

Glass composition (30-x)TeO₂-30B₂O₃-10ZnO-30BaO-xPr₂O₃ x = 0.00, 0.05, 0.10, 0.50, 1.00, and 1.50 mol% were fabricated using conventional melt quenching technique. In order to explore their structural and luminescence behavior, we measured the density, refractive index of the glass which shows increasing trend with increase in Pr₂O₃ concentration, also FTIR and XRD spectrum were analyzed to study the structural properties of the developed glasses. XRD shows amorphous structure of the prepared glasses. FTIR shows B-O stretching (BO₃) units and symmetrical stretching vibration of Te-O in TeO₄. The electronic states belonging to the 4f configuration of trivalent Pr³⁺ were determined from the absorption spectra. Multiphonon decay rate (W_{mp}), electron-phonon coupling strength (g) and host dependent parameter (α) were measured for the present glasses. The excitation spectra of the Pr doped glass samples were monitored at 605 nm. In the PL spectra, the characteristic emission bands due to *f-f* transition of Pr³⁺ were confirmed for the glass system, the highest transition ³P₀ → ³H₄ and ¹D₂ → ³H₄ corresponding to 589 nm and 605 nm respectively shows increase in intensity at 0.1 mol% concentration of Pr₂O₃.

1. Introduction

Glasses have unique characteristics such as glass transition and insulators these are optically transparent. One among several glass former, TeO₂ is one of the potential candidate for fabricating in fiber optical amplifiers, nonlinear optical glasses for telecommunication and also possess low phonon energy around 800 cm⁻¹ [1]. TeO₂ glass show far distance electromagnetic transmission (typically 300–5000 nm), high refractive indices. TeO₂ glasses also a good former which show high solubility when doped with rare earths [1,2], addition of various oxides would increase its glass forming range [3]. Due practical productivity of tellurite glasses, they grabbed attention of researcher to combine with borates to form borotellurite glasses, due their better transparency and refractive indices [4]. Boron oxide B₂O₃ is a basic

glass former due to its higher bond length, lower cation size, smaller heat of fusion and trivalence nature of boron. These glasses acquire units of triangular BO₃ units and tetragonal BO₄ units of borates which are corner bonded in a random fashion [5,6]. Zinc tellurite glasses represent one of the best potential host materials for several rare earth dopants for laser applications, addition of ZnO in such glasses would provide more homogenous amorphous nature by reducing their crystallizing state, better capability to form glasses and better constancy in their network [4]. ZnO has an advantage due their network forming as well as modifying capability when enters glass network. It also provides multifunctional material applications due availability of extensive band gap which can tailor the structural properties. Spectroscopic properties have received a great deal of interest, especially doping with rare-earth has improvised

the subject area much more interesting and potent on luminescence characteristics studies due 4f-4f intra interactions. Most oxide glasses have large phonon energy (1100 cm^{-1}) due to the stretching vibration of network-forming oxides [7], advantageous features of borate (high phonon energy $\sim 1200 - 1500\text{ cm}^{-1}$) and tellurite (low phonon energy $\sim 700 - 800\text{ cm}^{-1}$) glasses in their interactions with RE ions, could lead to low phonon energy and easy fabrication. Telecommunication application with praseodymium doped glasses has seen wide scope of interest so called second telecom window due their $1.3\ \mu\text{m}$ emission. They also exhibit 4 level lasing allied with $^3\text{P}_0$ level [8]. Most of the rare earths show visible emission while fewer among them such as Nd, Pr, Dy show $1.3\ \mu\text{m}$ NIR emission [9]. Praseodymium can show both visible and NIR emission, in present study we have chosen to explore its visible range emission. Pr^{3+} doped glasses restricted by diminutive lifetime. Few host glasses show volunteered oxidation of Pr^{3+} to form Pr^{4+} [10], following vitrification providing thrust emission intensity. However, quantum yield of Pr^{3+} is feeble in crystalline case [11]. Lifetime decay of f transition being instantly fast upto 13ns in silicate glasses doped with Pr^{3+} [12-15], such requirements advances them to applied solid state scintillating applications. Therefore, we have preferred to fabricate barium zinc boro-tellurite glasses doped with Pr^{3+} ions to study their behavior in optical properties.

2. Experimental

$(30-x)\text{TeO}_2-30\text{B}_2\text{O}_3-10\text{ZnO}-30\text{BaO}-x\text{Pr}_2\text{O}_3$ (ZTB) $x = 0.00, 0.05, 0.10, 0.50, 1.00, 1.50$ mol% were synthesized by usual melt-quench scheme. Analytical grade TeO_2 , H_3BO_3 , ZnO , BaO & Pr_2O_3 with high purity up to 99.99% were used as starting batch materials. These oxides were weighed using digital weighing machine with an accuracy of $\pm 0.001\text{ g}$, these chemicals were mixed thoroughly and then put in a furnace for melting using alumina crucible. The batches were melted at 1000°C and hold for 3 h. After melting the chemical melt were poured on a pre heated brass mold for quenching. The quenched samples were placed in another furnace at 300°C for annealing purposes due releases any thermal stress present. After annealing, the samples were taken out of furnace, subsequently

cut and polished with required dimensions. The refractive index of the glass samples was determined by Abbe refractometer (ATAGO Co. Ltd - 2016) at sodium wavelength (589.3 nm) using mono-bromo-naphthelene as contact fluid. By using Archimedes principle, density was measured. Structural analysis measured using Agilent Cary 630 FTIR spectrometer and sample were powdered to acquire fine powder for X-ray diffraction (XRD) measurements using Shimadzu Diffractometer XRD-6100 with $\text{Cu K}\alpha$ radiation source with 40 kV, 30 mA, Schimadzu-3600 spectrometer to measure UV-Vis-NIR spectra in 200 nm to 2500 nm wavelength region. The photoluminescence spectra were obtained by Cary-Eclipse fluorescence spectra. Color of emission is studied via CIE (Commission International de l'Eclairage 1931) chromaticity diagram.

3. Results and discussion

3.1 Physical properties

The structural changes and configuration is an important tool to understand the glass network [16]. From Figures 1a and 1b the density (ρ) and refractive index (n) increases by means of increase in Pr_2O_3 content, whereas molar volume decreases. Increase in density and decrease in molar volume indicates better compactness of the glass due increase of bridging oxygen's (BO's), i.e., non-bridging oxygen's (NBO's) present in $[\text{BO}_3]^{3-}$ triangles convert into bridging oxygen's of BO_4^- tetrahedral units with addition of Pr_2O_3 content. This leads to increase in the rigidity of the prepared glasses and also affects the indices of refractive (n) of the present ZTB glasses.

3.2 XRD studies

From Figure 2 for all ZTB glasses, shows no discrete or sharp diffraction lines. This confirms the amorphous nature of Pr_2O_3 doped ZTB glasses. The X-ray diffraction traces for all glass system were measured at room temperature and found to show almost similar trends. The measurement was performed using 2θ Vs intensity ranging from 10° to 80° with in steps of 0.02° with 1s as counting rate per step with speed of $5^\circ\cdot\text{min}^{-1}$.

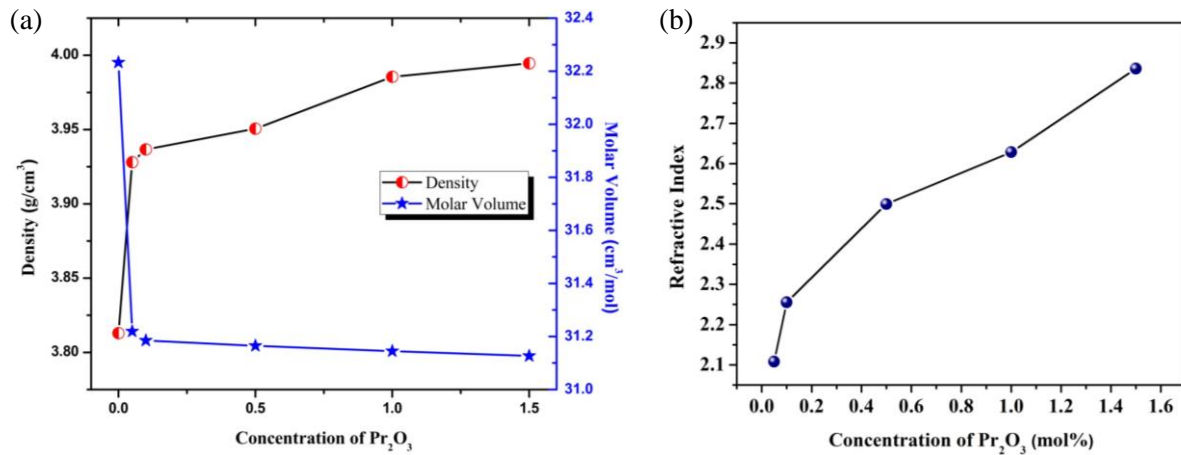


Figure 1. (a) Density, molar volume vs Pr₂O₃ concentration and (b) refractive index vs Pr₂O₃ concentration.

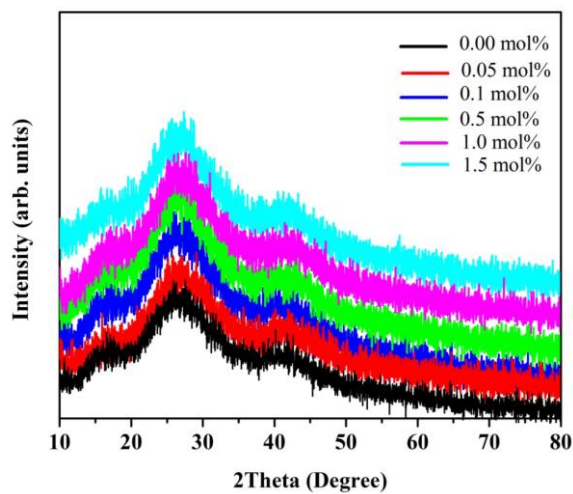


Figure 2. XRD of ZTB doped with Pr₂O₃ concentration.

3.3 FTIR studies

The Fourier Transform Infrared spectrum of zinc boro-tellurite (ZTB) doped with Pr₂O₃ glass were analyzed in range 650–2600 cm⁻¹ as displayed in Figure 3, the bands were assigned in Table 1. FTIR diagram shows the distinctive IR interest band at ~2080–2287 cm⁻¹ [17,18], ascribed to the elemental vibrations of OH group. Phonon energy being related to non-radiative loses, as phonon energy could be increased due occurrence of large amount of OH content, hence FTIR studies is important tool to study. The low intensity of OH band seen for ZTB glasses indicating the presence of low OH content leading to weaken borate phonon bands. The peak observed at 660 cm⁻¹ is due to the Te_{eq}-

O_{ax}-Te linkages [19–21]. The peak observed at 781 cm⁻¹ is due to the shaking of unbroken arrangement collected of TeO₄ trigonal bipyramids (tbp's) [19]. This band illustrate wide enough due addition of borate and also shows feeble vibration arising from BO₃ triangles [22]. The band arising at 1183 cm⁻¹ is due to elastic (stretching) shaking (vibrations) of BO₄ units present in the present glasses, as discussed in section 3.1 it can be noticed that the intensity of 1183 cm⁻¹ increases with increase in Pr₂O₃ concentration indicating that available NBO's (Non-Bridging Oxygen's) convert to BO's (Bridging Oxygen's). A supplementary very faint band arises in the spectrum of borate glasses around 1540 cm⁻¹, which is assumed to be B-O elastic shaking of BO₃ units with (BØ₂O) and without non-bridging oxygen ions [19,22–25].

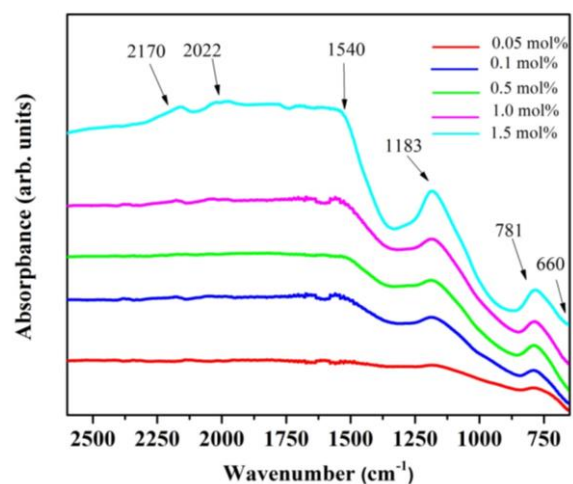


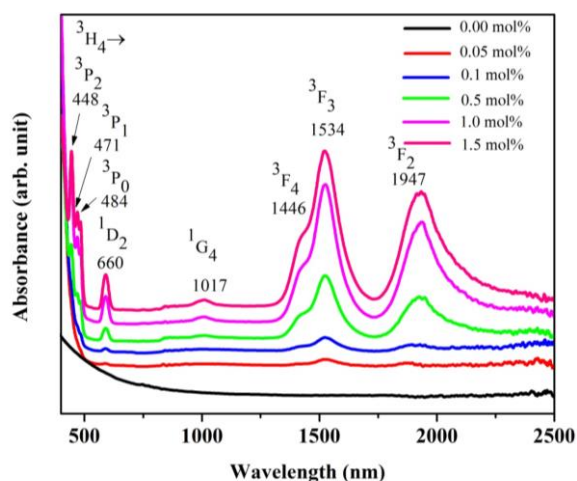
Figure 3. FTIR of ZTB doped with Pr₂O₃ concentration.

Table 1: FTIR absorption band assignments for ZTB glass samples.

Band Assignments [19-25]	Range (cm ⁻¹)	Wavenumber (cm ⁻¹)
Hydroxyl O-H stretching OH groups		2022 2170
B-O stretching vibrations of BO ₃ units with (B \bar{O} ₂ O) and without nonbridging oxygen ions	1520 - 1580	1540
Elastic (stretching) shaking (vibrations) of BO ₄ units	1160 - 1240	1183
TeO ₄ trigonal bipyramids (tbp's)	760 - 800	781
Te _{eq} -O _{ax} -Te linkages	650 - 680	660

3.4 Absorption studies

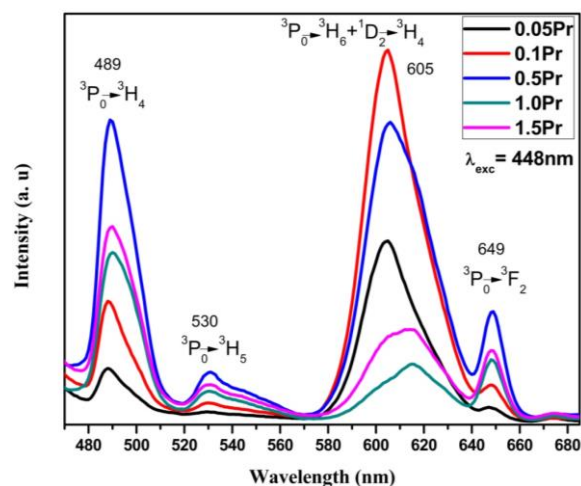
The prepared glasses were well polished to shiny glossy finish for spectroscopic quantification. Absorption spectra of Pr³⁺-doped ZTB glass samples were quantified in the visible and near-infrared NIR regions at room temperature on a dual beam spectrophotometer. Figure 4 shows eight absorption bands peaking at 446, 471, 484, 660, 1017, 1446, 1534 and 1947 nm associated with the absorption transitions from the ground state ³H₄ to ³H₄ → ³P₂, ³H₄ → ³P₁, ³H₄ → ³P₀, ³H₄ → ¹D₂, ³H₄ → ¹G₄, ³H₄ → ³F₄, ³H₄ → ³F₃ and ³H₄ → ³F₂ respectively to the specific excited states as displayed in the Figure 4.

**Figure 4.** UV-Vis-NIR spectra of ZTB doped with Pr₂O₃ concentration.

3.5 Luminescence studies

The emission spectra of the ZTB glass samples monitored at 448 nm excitation wavelength are presented in Figure 5. Pr³⁺ owns a variety of radiative changeovers from ³P₀ and ¹D₂ levels when

excited by blue light. Four emission bands located at 489, 530, 605, and 649 nm corresponding to ³P₀ → ³H₄, ³P₁ → ³H₅, ³P₀ → ³H₆ + ¹D₂ → ³H₄ and ³P₁ → ³F₂ transitions of Pr³⁺ are obtained under 448 nm excitation. Due to the large energy gap (3757 cm⁻¹) between ³P₀ and ¹D₂ and the observed phonon energy from FTIR (1183 cm⁻¹), multiphonon nonradiative relaxation from ³P to ¹D₂ is very small, and hence the ¹D₂ luminescence was not observed. Highest emission intensity found at 0.1 mol% which reveals that concentration quenching occurs at 0.1 mol% Pr₂O₃ content.

**Figure 5.** Emission spectra of ZTB doped Pr₂O₃ concentration.

Among all these transitions, two transitions are highly intense in bluish-green and bright red regions at 489 nm and 605 nm corresponding to the transitions ³P₀ → ³H₆ + ¹D₂ → ³H₄ for ZTB glass. These two transitions are originating from ³P₀ and ¹D₂ and they are well resolved. The bluish-green emission from Pr³⁺ ions doped ZTB glasses can be explained on the basis of its energy level structure. The energy gap between ³P₀ and ¹D₂ is 4042 cm⁻¹. In the present series of glasses, orange-red

luminescence dominates bluish-green luminescence because of non-radiative relaxation that took place from ³P₀ to ¹D₂. In case of 0.5 mol% doped Pr₂O₃ in ZTB glass shows ³P₀ → ³H₄ transition (489 nm) bluish-green luminescence dominating than the orange luminescence because of increased radiative transition from ³P₀ to ground state instead of non-radiative relaxation of ³P₀ to ¹D₂ state, whereas for 0.1 mol% doped Pr₂O₃ in ZTB glass shows ¹D₂ → ³H₄ transition (605 nm) orange luminescence dominating than the bluish-green indicating non-radiative relaxation (multi phonon relaxation) of ³P₀ to ¹D₂ state is quite strong.

The excitation spectra of the ZTB glass samples monitored at 605 nm are displayed in Figure 6. The excitation bands peaking at 447, 472, and 485 nm are assigned to the absorption transitions of ³H₄ → ³P₂, ³H₄ → (¹I₆, ³P₁), and ³H₄ → ³P₀, respectively, signifying that the emissions emanating from ³P₀ and ¹D₂ states attained under such excitation are viable blue laser diode, blue and blue-greenish LEDs. The energy level illustration is shown in Figure 7 for the prepared glass samples doped with Pr³⁺ ions. The concentration quenching was observed at 0.1 mol% of Pr₂O₃ content as the distance between Pr³⁺-Pr³⁺ decreases as concentration increases beyond 0.1 mol%. Using 448 nm excitation wavelength the exciton is excited to ground state of higher level through non-radiative transition, this excitation de-excited to excited level of ground state (³P₀). From ground state of higher excited state, we observe four emission bands located at 489 nm (blue), 530 nm (green), 605 nm (orange) and 649 nm (red) as shown in Figure 7. The multiphonon tranquility rate (*W_{mp}*) between the excited level to the next lower level can be expressed by the Miyakawa-Dexter equation [26],

$$W_{mp} = W_o \exp(-\alpha\Delta E/\hbar\omega) \quad (1)$$

where

$$\alpha = \frac{1}{\hbar\omega} \left[\ln \left(\frac{p}{g(n+1)} \right) - 1 \right] \quad (2)$$

where α and W_o are the experimentally determined constraint which are constant for a given host. Also the constraint W_o match up to the decay rate at zero energy gap and g is the electron-phonon coupling strength. In the current work, the phonon energy

($\hbar\omega$) of ZTB glass is about 1183 cm⁻¹, p is the quantity of phonons essential to bridge the energy gap ($\Delta E = 3757$ cm⁻¹) between the excited and the next lower level, minimum of six phonons (calculated $p = 6$) are required for bridging the ³P₀→¹D₂ multiphonon relaxation process. The partition distribution function (n) for the population of phonons as a function of temperature (T) and $\hbar\omega$ can be expressed as

$$n = \left(e^{\frac{\hbar\omega}{kT}} - 1 \right)^{-1} \quad (3)$$

An significant supply for high quantum efficiency is a extended total lifetime, attained by decreasing the non-radiative decay rate hence, multiphonon decay rate of a excited level is resolved by the phonon energy of the host, and is greatly lessened in low phonon energy glasses. Equations (1-3) above are a phenomenological affiliation which allows to gauge the anticipated multiphonon decay rate from the known energy gap of the ion and the phonon energy of the host [26,27], Considering in account of two formers present in the glass system and from FTIR data, it was found that for the W_{mp}/W_o for ³P₀→¹D₂ in the present boro-tellurite is found to 0.986, electron-phonon coupling strength g is found to be 0.0131 and host dependent parameter α is found to be 4.269×10⁻³ cm, which proposes that these values are comparable and one may expect the longer lifetime and quantum efficiency [28,9].

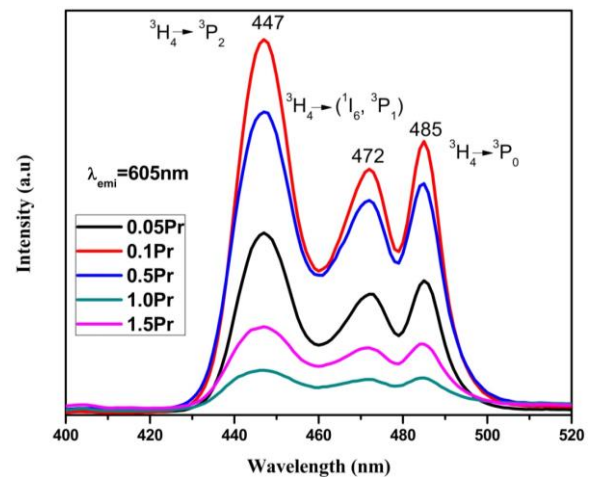


Figure 6. Excitation spectra of ZTB doped Pr₂O₃ concentration.

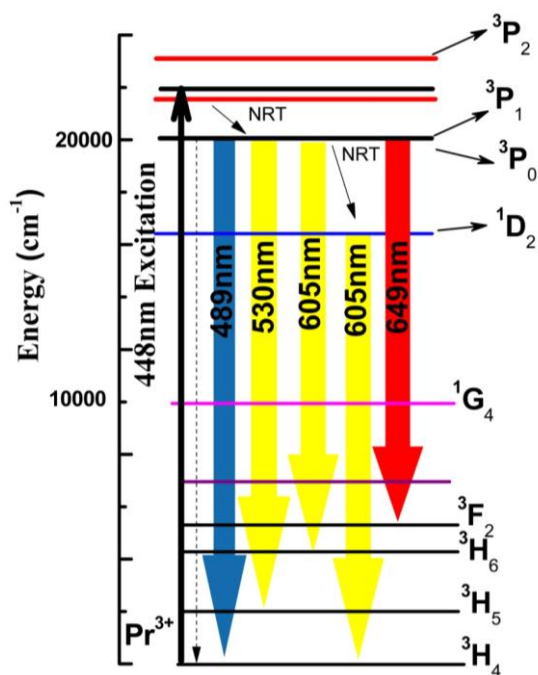


Figure 7. Energy level diagram of ZTB doped Pr_2O_3 concentration.

3.6 CIE Chromaticity studies

The three dimensionless coordinates " $\bar{x}(\lambda)$; $\bar{y}(\lambda)$; $\bar{z}(\lambda)$ " are used to portray the color from any light source [29-31]. The Commission International de l'Éclairage (CIE) chromaticity coordinates are resolved from the tristimulus values to approximate the emission color of the glass matrices through the given relations

$$x = \frac{X}{X+Y+Z} \quad (4)$$

$$y = \frac{Y}{X+Y+Z} \quad (5)$$

The circumference of CIE1931 chromaticity diagram is prepared by particular position of all monochromatic color coordinates while the zone is compiled of all the multi chromatic wavelengths. The color coordinates of the multi-colored fluorescence in ZTB glasses under the assorted excitation conditions are developed and spotted on the CIE-1931 customary chromaticity diagram. A multi-color integral fluorescence originated from the combination of the residual laser and the Pr^{3+} spontaneous emission which can be recognized by adjusting the intensity ratio between the laser and the Pr^{3+} emissions as shown in Figure 8. The CIE 1931 color coordinates for the fluorescence of the 0.1 mol% Pr^{3+} doped zinc boro-tellurite glasses

under 448 nm laser excitation conditions, whose color coordinate is derived to be $\sim(0.332, 0.611)$ corresponding to yellow-green.

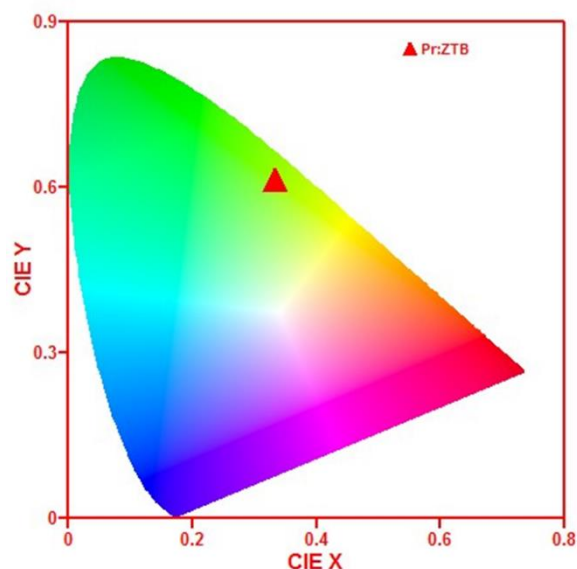


Figure 8. Color coordinates in the CIE 1931 chromaticity diagrams for 0.1 mol% of Pr_2O_3 doped ZTB glasses under 448 nm laser excitation.

4. Conclusions

The Pr^{3+} doped zinc boro-tellurite glasses were synthesized by usual melt-quench scheme. Enhancement in density, refractive index and decline in molar volume of these ZTB glasses indicates that these glasses show enhancement in their compactness of the glass structure. Amorphous environment of the glass was substantiated by XRD measurements. Structural investigation from FTIR reveals that TeO_3 trigonal pyramids and BO_4 units are present in these glasses. Four emission bands were observed at 489, 530, 605, and 649 nm corresponding to Pr^{3+} ion monitoring at 448 nm excitation and found that concentration quenching at 0.1 mol% Pr_2O_3 . Calculations were made to calculate multiphonon tranquility rate W_{mp}/W_0 for ${}^3\text{P}_0 \rightarrow {}^1\text{D}_2$ in the present boro-tellurite is found to 0.986, electron-phonon coupling strength g is found to be 0.0131 and host dependant parameter α is found to be 4.269×10^{-3} cm, indicating that extended lifetimes could be feasible in low phonon energy glasses. The CIE chromaticity color co-ordinates are measured which is $\sim(0.332, 0.611)$ corresponding to yellow-green.

5. Acknowledgments

The instigator shows gratitude towards National Research Council of Thailand (NRCT) and Nakhon Pathom Rajabhat University (NPRU) for supporting to delve such investigations. R. Rajaramakrishna is grateful to his advisor (J. Kaewkhao) and NPRU for granting project (Grant number PD1_2017).

References

- [1] L. D. Vila, L. Gomes, C. R. Eyzaguirre, E. Rodriguez, C. L. Cesar, and L. C. Barbosa, "Time resolved luminescence in (T_m:H_o) doped tellurite glass," *Optical Materials*, vol. 27, pp.1333–1339, 2005.
- [2] N. B. Shigihalli, R. Rajaramakrishna, and R. V. Anavekar, "Optical and radiative properties of Nd³⁺-doped lead tellurite borate glasses," *Canadian Journal of Physics*, vol.91, pp. 322-327, 2013.
- [3] N. Manikandan and A. Rysanyanskiy, J. Toulouse, "Thermal and optical properties of TeO₂-ZnO-BaO glasses," *Journal of Non-Crystalline Solids*, vol. 358, pp. 947–951, 2012.
- [4] N. B. Shigihalli, R. Rajaramakrishna, and R. V. Anavekar, "Optical properties of Eu³⁺ doped lead borate tellurite and zinc borate tellurite glasses," *AIP Conference Proceedings*, vol. 1349, pp. 547-548, 2011.
- [5] R. Rajaramakrishna, S. Karuthedath, R. V. Anavekar, and H. Jain, "Nonlinear optical studies of lead lanthanum borate glass doped with Au nanoparticles," *Journal of Non-Crystalline Solids*, vol. 358, pp. 1667–1672, 2012.
- [6] R. Rajaramakrishna, C. Saiyasombat, R. V. Anavekar, and H. Jain, "Structure and nonlinear optical studies of Au nanoparticles embedded in lead lanthanum borate glass," *Journal of Non-Crystalline Solids*, vol. 406, pp. 107–110, 2014.
- [7] Z. A. Said Mahraz, M. R. Sahar, and S. K. Ghoshal, "Band gap and polarizability of boro-tellurite glass: Influence of erbium ions," *Journal of Molecular Structure*, vol. 1072, pp. 238–241, 2014.
- [8] K. Annapurna, R. Chakrabarti, and S. Buddhudu, "Absorption and emission spectral analysis of Pr³⁺ tellurite glasses," *Journal of Materials Science*, vol. 42, pp. 6755–6761, 2007.
- [9] M. Naftaly, A. Jha, and W. G. Jordan, "1.3 μm fluorescence quenching in Pr-doped glasses," *Journal of Applied Physics*, vol. 84, pp. 1800-1804, 1998.
- [10] A. Mekki, Kh. A. Ziq, D. Holland, and C. F. Mc Conville, "Magnetic properties of praseodymium ions in Na₂O-Pr₂O₃-SiO₂ glasses," *Journal of Magnetism and Magnetic Materials*, vol. 260, pp. 60–69, 2003.
- [11] X. Wang, S. Huang, L. Lu, and W. M. Yen, "Measurement of quantum efficiency in Pr³⁺-doped CaAl₄O₇CaAl₄O₇ and SrAl₄O₇SrAl₄O₇ crystals," *Applied Physics Letters*, vol. 79, pp. 2160–2612, 2001.
- [12] Y. Sun, M. Koshimizu, S. Kishimoto, and K. Asai, "Synthesis and characterization of Pr³⁺-doped glass scintillators prepared by the sol-gel method," *Journal of Sol-Gel Science and Technology*, vol. 62, pp. 313–318, 2012.
- [13] H. Tawarayama, E. Ishikawa, K. Yamanaka, K. Itoh, K. Okada, H. Aoki, H. Yanagita, Y. Matsuoka, and H. Toratani, "Optical Amplification at 1.3 μm in a Praseodymium-Doped Sulfide-Glass Fiber," *Journal of the American Ceramic Society*, vol. 83, pp. 792-796, 2000.
- [14] D. T. Schaafsma, L. B. Shaw, B. Cole, J. S. Sanghera, and I. D. Aggarwal, "Modeling of Dy³⁺-doped GeAsSe glass 1.3-μm optical fiber amplifiers," *IEEE Photonics Technology Letters*, vol. 10, pp. 1548-1550, 1998.
- [15] Y. G. Choi, K. H. Kim, B. J. Park, and J. Heo, "1.6 μm emission from Pr³⁺: (3F₃, 3F₄) → 3H₄Pr³⁺: (3F₃, 3F₄) → 3H₄ transition in Pr³⁺ - and Pr³⁺/Er³⁺-doped selenide glasses," *Applied Physics Letters*, vol. 78, pp. 1249, 2001.
- [16] B. Bhatia, S. L. Meena, V. Parihar, and M. Poonia, "optical properties of Nd³⁺-doped bismuth borate glasses," *New Journal of Glass and Ceramics*, vol. 5, pp. 44–52, 2015.
- [17] H. Ebendorff-Heidepriem, W. Seeber, and D. Ehrt, "Dehydration of phosphate glasses," *Journal of Non-Crystalline Solids*, vol. 163, p. 74, 1993.
- [18] S. Mahamuda, K. Swapna, P. Packiyaraj, A. S. Rao, and G. V. Prakash, "Visible red, NIR and Mid-IR emission studies of Ho³⁺ doped Zinc Alumino Bismuth Borate glasses," *Optical Materials*, vol. 36, p. 362, 2013.

- [19] P. Damas, J. Coelho, G. Hungerford, and N. S. Hussain, "Structural studies of lithium boro tellurite glasses doped with praseodymium and samarium oxides," *Materials Research Bulletin*, vol. 47, pp. 3489–3494, 2012.
- [20] R. Stegeman, C. Rivero, K. Richardson, G. Stegeman, P. Delfyett Jr., Y. Guo, A. Pope, A. Schulte, T. Cardinal, P. Thomas, and J. C. Champarnaud-Mesard, "Raman gain measurements of thallium-tellurium oxide glasses," *Optics Express*, vol. 13, p. 1144, 2005.
- [21] M. D. Pankova, Y. Dimitriev, V. Arnaudov, and V. Dimitrov, "Infrared spectral investigation of the influence of modifying oxides on the structure of tellurite glasses," *Journal of Physical Chemistry*, vol. 30, pp. 260-263, 1989.
- [22] E. I. Kamitsos, M. A. Karakassides, and G. D. Chryssikos, "A vibrational study of lithium borate glasses with high Li₂O content," *Physics and Chemistry of Glasses*, vol. 28, pp. 203-209, 1987.
- [23] E. I. Kamitsos, A. P. Patsis, M. A. Karakassides, G. D. Chryssikos, "Infrared reflectance spectra of lithium borate glasses," *Journal of Non-Crystalline Solids*, vol. 126, pp. 52-67, 1990.
- [24] E. I. Kamitsos and G. D. Chryssikos, "Borate glass structure by Raman and infrared spectroscopies," *Journal of Molecular Structure*, vol. 247, pp. 1-16, 1991.
- [25] H. Doweidar, G. El-Damrawi, K. El-Egili, and R. M. Ramadan, "Sites distribution and properties of Al₂O₃-PbO-B₂O₃ glasses," *European Journal of Glass Science and Technology Part B*, vol. 49, pp. 271-277, 2008.
- [26] T. Miyakawa and D. L. Dexter, "Phonon side bands, multiphonon relaxation of excited states and phonon-assisted energy transfer between ions in solids," *Physical Review B*, vol. 1, pp. 2961-2969, 1970.
- [27] G. F. Imbush, B. Di Bartolo, Ed., *Advances in Nonradiative Processes in Solids*, New York: Plenum, 1991, p. 261.
- [28] P. Manasa and C. K. Jayasankar, "Luminescence and phonon side band analysis of Eu³⁺-doped lead fluorosilicate glasses," *Optical Materials*, vol. 62, pp. 139-145, 2016.
- [29] K. Kirksiri, R. R. Ramakrishna, B. Damdee, H. J. Kim, S. Kaewjaeng, S. Kothan, and J. Kaewkhao, "Investigations of optical and luminescence features of Sm³⁺ doped Li₂O-MO-B₂O₃ (M=Mg/Ca/Sr/Ba) glasses mixed with different modifier oxides as an orange light emitting phosphor for WLED's," *Journal of Alloys and Compounds*, vol. 749, pp. 197-204, 2018.
- [30] I. Khan, G. Rooh, R. Rajaramakrishna, N. Srisittipokakun, H. J. Kim, C. Wongdeeying, and J. Kaewkhao, "Development of Eu³⁺ doped Li₂O-BaO-GdF₃-SiO₂ oxyfluoride glass for efficient energy transfer from Gd³⁺ to Eu³⁺ in red emission solid state device application," *Journal of Luminescence*, vol. 203, pp. 515–524, 2018.
- [31] I. Khan, G. Rooh, R. Rajaramakrishna, N. Srisittipokakun, C. Wongdeeying, N. Kiwsakunkran, N. Wantana, H. J. Kim, J. Kaewkhao, S. Tuscharoen, "Photoluminescence and white light generation of Dy₂O₃ doped Li₂O-BaO-Gd₂O₃-SiO₂ for white light LED," *Journal of Alloys and Compounds*, vol. 774, pp. 244-254, 2019.